

## Comparison of Dirac and Schrödinger descriptions of spin observables for proton-nucleus elastic scattering at 650 and 800 MeV

W. Rory Coker and L. Ray\*

*Department of Physics, The University of Texas at Austin, Austin, Texas 78712*

(Received 27 December 1989)

We compute the analyzing power,  $A_y$ , and spin rotation,  $Q$ , for proton elastic scattering at 650 and 800 MeV from target nuclei  $^{16}\text{O}$ ,  $^{40}\text{Ca}$ , and  $^{208}\text{Pb}$ , using both nonrelativistic multiple-scattering theory and a relativistic impulse approximation model. We show that the nonrelativistic theory, based on the Schrödinger equation with relativistic kinematics, and the relativistic model, based on the Dirac equation, provide very similar and equally good descriptions of these spin observables when electromagnetic spin-orbit contributions are included in both approaches. The nonrelativistic model calculations include contributions from nuclear medium effects (Pauli blocking and binding energy corrections) and also target nucleon two-body correlations. Medium effects and correlations are not expected to be significant in the relativistic model based on the Dirac equation, and were not included.

### I. INTRODUCTION

One of the major attractions of medium energy nuclear physics has been the possibility which it offers for the description of processes such as nucleon-nucleus scattering within a microscopic framework in which a multiple-scattering theory<sup>1,2</sup> is used to relate the nucleon-nucleus optical potential directly to nucleon-nucleon (NN) scattering phenomenology and to empirical or theoretical nuclear matter densities. Two major topics of discussion during the past decade have been the range of validity of the nonrelativistic impulse approximation (NRIA), and the importance of relativistic dynamics, in proton-nucleus elastic scattering.<sup>3-7</sup> Particular attention has been focused on the spin observables: the analyzing power,  $A_y$ , and the spin-rotation parameter,  $Q$ . It has been repeatedly shown that lowest-order nonrelativistic impulse approximation calculations, based on the Schrödinger equation with relativistic kinematics, meet with severe difficulty in describing the experimental data for  $A_y$  and  $Q$  for all incident energies, up to and including 1 GeV.<sup>4-8</sup> During the past few years it has been demonstrated that the use of a relativistic version of the impulse approximation—the so-called relativistic impulse approximation, or RIA—accompanied by solution of the Dirac equation, provide a dramatically better overall description of  $A_y$  and  $Q$ , at least at incident energies higher than 400 MeV.<sup>4,5</sup>

However, at 800 MeV the relativistic approach exhibits in its predictions of differential cross sections and spin observables an unrealistic and vexing target mass dependence.<sup>8</sup> Furthermore, both relativistic and nonrelativistic impulse approximation approaches fail at the lower energies, below 400 MeV. The lower-energy predictions of both approaches may be improved dramatically by explicitly accounting for projectile-target nucleon exchange, and by using an effective interaction that takes into account the nuclear medium.<sup>6,7,9</sup> The lower-energy

predictions of the relativistic calculations are generally satisfactory provided the pseudovector, rather than pseudoscalar, form of the NN Lorentz invariant amplitudes is assumed.<sup>6,7</sup>

It is customary in the literature to compare the predictions of the RIA model with those of the simplest, first-order NRIA calculations in order to elucidate the contributions of the virtual pair terms.<sup>4-7</sup> However, for heavy target nuclei at higher intermediate energies, this sort of comparison is flawed because the RIA inherently includes a portion of the electromagnetic coupling of the incident proton magnetic moment, while it is usually completely excluded from the NRIA. Also, in recent years, a number of important corrections to the impulse approximation have been worked out within the NR model.<sup>8,10</sup> It is therefore timely to compare the RIA predictions and the available data with NR predictions which include recent improvements, and to account properly for magnetic moment coupling in both models.

In this work we will focus on the higher energies and demonstrate the following two points. First, at 650 and 800 MeV, for nuclear targets of medium to heavy mass, the success of the RIA-Dirac equation approach, as compared to that of the usual NRIA calculation, is due in part to the implicit inclusion in the Dirac approach of the electromagnetic spin-orbit interaction depending upon the magnetic moment of a pointlike, spin- $\frac{1}{2}$  “Dirac proton” projectile. Second, when spin-orbit effects due to the actual, full proton magnetic moment are accounted for in both approaches, and when target nucleon correlations and medium corrections<sup>10</sup> are further included in the NR model, both approaches provide similar and generally accurate descriptions of the 650- and 800-MeV spin observable data for proton elastic scattering from  $^{16}\text{O}$ ,  $^{40}\text{Ca}$ , and  $^{208}\text{Pb}$ .

The portion of the nucleon-nucleus electromagnetic interaction that involves the projectile magnetic moment automatically appears in the Dirac approach, but also

occurs quite naturally in the nonrelativistic approach.<sup>11</sup> It has tended to be omitted in almost all nonrelativistic calculations done to date because of accompanying numerical difficulties. In the following we show that, within the framework of the two models under consideration here, the electromagnetic spin-orbit (EMSO) potential is indispensable in obtaining a satisfactory description of the spin observables  $A_y$  and  $RQ$  for proton-nucleus elastic scattering at 650 and 800 MeV, at small scattering angles, except for light target nuclei.

The elements of the calculations are briefly reviewed in the next section. The results are presented and discussed in Sec. III; a summary of the conclusions is given in Sec. IV.

## II. CALCULATIONAL DETAILS

### A. Nonrelativistic approach

The ingredients of the first-order multiple-scattering description of the local proton-nucleus optical potential are free proton-nucleon scattering amplitudes,  $f$ , and ground-state nuclear matter densities. For the nonrelativistic calculations, the proton matter densities  $\rho_p(r)$  were unfolded from the empirically known charge densities,<sup>12-14</sup> while the neutron matter densities were constructed according to the recipe

$$\rho_n(r) = \rho_p(r) + [\rho_n^{\text{HFB}}(r) - \rho_p^{\text{HFB}}(r)], \quad (1)$$

where the densities  $\rho^{\text{HFB}}$  were obtained from the Hartree-Fock-Bogoliubov (HFB) calculations of Dechargè and Gogny.<sup>15</sup>

Proton-nucleon scattering amplitudes were obtained from the recent SP89 phase-shift solution.<sup>16</sup> The proton-nucleon scattering amplitudes needed for the calculations will be discussed in the Wolfenstein form,

$$f = a + b(\sigma_{1n} - \sigma_{2n}) + c(\sigma_{1n} + \sigma_{2n}) + m\sigma_{1n}\sigma_{2n} \\ + (g + h)\sigma_{1p}\sigma_{2p} + (g - h)\sigma_{1q}\sigma_{2q}, \quad (2)$$

where subscripts 1 and 2 refer to the two nucleons, and  $a$ ,  $b$ ,  $c$ ,  $m$ ,  $g$ , and  $h$  are complex amplitudes which are functions of momentum transfer  $q$ . For incoming center-of-momentum system nucleon wave number  $\mathbf{k}$  and outgoing wave number  $\mathbf{k}'$ , the direction of  $\mathbf{q}$  is given by  $\hat{\mathbf{q}} = (\mathbf{k} - \mathbf{k}')/|\mathbf{k} - \mathbf{k}'|$ . The notation  $\sigma_{1j}$  means  $\sigma_{1 \cdot \hat{\mathbf{j}}}$ ; the other two unit vectors appearing in Eq. (2),  $\hat{\mathbf{n}}$  and  $\hat{\mathbf{p}}$ , are defined as usual by  $\hat{\mathbf{p}} = (\mathbf{k} + \mathbf{k}')/|\mathbf{k} + \mathbf{k}'|$  and  $\hat{\mathbf{n}} = (\mathbf{k} \times \mathbf{k}')/|\mathbf{k} \times \mathbf{k}'|$ .

For elastic scattering of protons from spin-zero target nuclei, amplitudes  $a(q)$  and  $c(q)$  make the predominant contribution to the nuclear part of the proton-nucleus optical potential. Amplitude  $a(q)$  for  $p+p$  contains a purely Coulombic term (in lowest order, a Rutherford amplitude behaving like  $1/q^2$  at small  $q$ ), which leads in the impulse approximation to the usual proton-nucleus Coulomb potential. It is usual to suppress the Coulombic part of  $a$  and calculate the Coulomb potential directly from the empirical nuclear charge distribution.<sup>17</sup> The electromagnetic contribution to amplitudes  $b$  and  $c$  (it is the same for both amplitudes) behaves like  $1/q$  at small  $q$

and arises from the interaction of the nucleon's magnetic moment with a current due to the momentum of the proton.<sup>18</sup> For  $p+p$  scattering, particle identity requires amplitude  $b$  to vanish, and charge independence requires that the nuclear part of  $b$  also be zero for  $p+n$  scattering. For  $p+n$  the electromagnetic parts of amplitudes  $b$  and  $c$  combine in such a way that the electromagnetic contribution to the  $\sigma_p \cdot \hat{\mathbf{n}}(\sigma_N \cdot \hat{\mathbf{n}})$  term is zero (nonzero) where  $P(N)$  denotes a proton (neutron).<sup>11</sup>

However, for a spin-zero target, contributions from  $\sigma_N \cdot \hat{\mathbf{n}}$  terms in the  $p+n$  amplitude, and the target proton  $\sigma_p \cdot \hat{\mathbf{n}}$  term in the  $p+p$  amplitude, do not contribute to the first-order proton-nucleus spin-orbit optical-model potential. The principal contribution is from the projectile proton  $\sigma_p \cdot \hat{\mathbf{n}}$  part of the NN amplitudes. Thus, the proton-nucleus electromagnetic spin-orbit potential originates predominantly from the electromagnetic part of the amplitude  $c(q)$  for  $p+p$ . The  $1/q$  dependence of  $c$  results in an electromagnetic spin-orbit potential which falls off like  $1/r^3$  as  $r \rightarrow \infty$ , asymptotic behavior which leads to gross convergence difficulties unless one solves the dynamical equation containing it out to very large distances before matching to ordinary Coulomb solutions. Because of this, the electromagnetic contribution to the spin-orbit potential has almost invariably been omitted in NRIA calculations of  $p+nucleus$  observables. However, it is important to realize that solutions of the Dirac equation automatically include the electromagnetic spin-orbit contribution due to the spin- $\frac{1}{2}$  point particle portion of the proton's full magnetic moment. The remaining contribution, from the anomalous portion of the proton's magnetic moment, is readily included in the Dirac equation as a tensor term<sup>19</sup> and has usually been incorporated in proton-nucleus calculations.<sup>8,20</sup>

Often in the literature, the predictions of the relativistic impulse approximation model have been compared to NR multiple-scattering calculations which make use of a simple, first-order microscopic optical potential.<sup>1,2</sup> Because a major strength of the nonrelativistic approach is the consistent framework it provides, within which higher-order terms and corrections to the impulse approximation can be calculated, omission of such corrections as well as the electromagnetic spin-orbit potential when making comparisons to Dirac results can easily give a misleading impression of inherent difficulties with the nonrelativistic approach.

The first-order Watson<sup>2</sup> optical potential is given by the space Fourier transform of

$$U_{\text{opt}}^{(1)}(q) = \sum_{i=p,n} t_{pi}(q) \bar{\rho}_i(q), \quad (3)$$

where  $t_{pi}(q)$  is the on-shell  $t$ -matrix corresponding to the proton- $i$ th nucleon scattering amplitude  $f$ , Lorentz-transformed into the proton-nucleus center-of-momentum system assuming Breit frame kinematics,<sup>5</sup> and  $\bar{\rho}_i(q)$  is the Fourier transform of the matter density  $\rho_i(r)$ . The usual Coulomb potential is included but the electromagnetic spin-orbit term is customarily omitted. Examples of such calculations are shown in Ref. 5.

For comparison to Dirac results in this work, we present results of two types of NR calculations, differing

only in the inclusion or omission of the electromagnetic spin-orbit potential. However, in this work, we have included two corrections to the first-order, impulse approximation optical potential in both sets of NR calculations. The first correction accounts for Pauli, short-range dynamical and center-of-mass two-body correlations in the target nucleus state function<sup>21</sup> and is included via a second-order contribution,  $U_{\text{opt}}^{(2)}$ , to Eq. (3). This correlation correction has fairly small effects on  $Q$  at all angles, but makes a noticeable reduction in the  $A_y$  predictions at the larger angles, and thus plays a role in achieving overall good descriptions of the  $A_y$  data. The second type of correction accounts for Pauli blocking of intermediate NN scattering states and the binding energy of the struck target nucleon, in terms of an effective, density-dependent nucleon-nucleon  $t$  matrix. This interaction was constructed by solving a nonrelativistic coupled-channels isobar model.<sup>10</sup> To obtain an effective, on-momentum-shell scattering amplitude dependent on the target-nucleon Fermi momentum  $k_F$ , based on the SP89 solutions, we used the recipe<sup>10</sup>

$$t(k_F) = t_{\text{SP89}}(0) + [t(k_F) - t(0)]_{\text{Isobar Model}}, \quad (4)$$

where  $k_F$  varies from 0.0 to  $1.36 \text{ fm}^{-1}$  as one moves from free space into the nuclear interior.

As shown in Ref. 10, inclusion of medium corrections (“density dependence”) tends to sharpen to some extent the weak structure in the NRIA predictions of  $A_y$  and  $Q$  at 650 and 800 MeV. At these energies, the most important medium effect is the binding energy correction, which does tend to move the predictions for  $A_y$  and  $Q$  toward the data, but still leaves the overall description of these observables in a rather poor state for all but the lighter target nuclei. In general, the NR density-dependent descriptions, including correlations, remain vastly inferior to those provided by the RIA calculations using the Dirac equation.<sup>5,8</sup> In the RIA-Dirac equation approach, correlation effects<sup>22</sup> and medium corrections<sup>6,7</sup> appear to be negligible, and thus were not included in the Dirac calculations reported here.

For the second set of NR model calculations, the electromagnetic spin-orbit potential was included in the Schrödinger equation using the approach discussed in Ref. 11. The first-order EMSO potential resulting from the impulse approximation has the asymptotic form

$$(U_{\text{EMSO}}/r^3)\sigma \cdot l, \quad (5)$$

with  $U_{\text{EMSO}}$  a complex number. It was multiplied by a Gaussian weighting factor  $\exp[-\alpha(r-r_{\text{SO}})^2]$ , and the observables  $A_y$  and  $Q$  were calculated as a function of parameter  $\alpha$ . The quantity  $r_{\text{SO}}$  was taken as about  $1.1 \text{ fm} \times A^{1/3}$ . The specific values of  $\alpha$  used in the calculations were 0.01, 0.02, and  $0.03 \text{ fm}^{-2}$ . The quantities  $A_y(\theta, \alpha)$  and  $Q(\theta, \alpha)$  were then extrapolated to  $\alpha=0$ . The relevant range of  $\alpha$ , and knowledge of the functional dependence on  $\alpha$  of  $A_y(\theta, \alpha)$  and  $Q(\theta, \alpha)$  necessary in extrapolating to  $\alpha=0$ , were obtained by performing Glauber<sup>23</sup> calculations for various values of  $\alpha$ , including  $\alpha=0$ , as discussed in Ref. 11. For  $^{208}\text{Pb}$ , the eikonal approximation becomes very unrealistic for angles greater

than  $15^\circ$ , and the Glauber calculations for  $A_y$  and  $Q$  could not be used as a guide to extrapolation; fortunately, no guide was required, since at these angles,  $Q$  and  $A_y$  for  $p + ^{208}\text{Pb}$  at 650 and 800 MeV are weak, smooth functions of  $\alpha$ .

With  $\alpha=0.01 \text{ fm}^{-2}$  the tail of the EMSO potential is still quite long and relatively large radii for matching to Coulomb solutions (about 20 fm), and many partial waves (110 to 145 depending upon target mass and incident energy) were used in the Schrödinger equation calculations. To give an idea of the size of the electromagnetic spin-orbit term, at 800 MeV the values of  $U_{\text{EMSO}}$  are, in  $\text{MeV}\cdot\text{fm}^3$  for  $p + ^{208}\text{Pb}$ ,  $^{40}\text{Ca}$ , and  $^{16}\text{O}$ , respectively,  $(-3.465, -0.244)$ ,  $(-0.874, -0.0622)$ , and  $(-0.372, -0.026)$ . For 650 MeV, the values, in the same order, are  $(-3.764, -0.249)$ ,  $(-0.945, -0.0678)$ , and  $(-0.398, -0.028)$ .

The NR calculations including correlations, medium effects and the electromagnetic spin-orbit potential are shown as solid curves in the figures. Corresponding NR calculations in which the EMSO potential is suppressed are shown as dash-dot curves. We have not included “off-shell” or “full-folding” corrections as recently discussed by several authors.<sup>24–27</sup> Such effects are presumably most important for lower energies and lighter nuclei; however, lack of adequate knowledge of the off-shell behavior of the nucleon-nucleon interaction at energies above 400 MeV makes estimates difficult.<sup>25</sup> The results of Ref. 27 suggest that at 650 and 800 MeV these additional corrections to the impulse approximation are expected to be rather small.

## B. Relativistic approach

The RIA-Dirac equation calculations presented here were based on the local form for the NN Lorentz-invariant amplitude of Ref. 3, given by

$$F = F_S + F_P \gamma_1^5 \gamma_2^5 + F_V \gamma_1^\mu \gamma_2^\mu + F_A \gamma_1^5 \gamma_1^\mu \gamma_2^5 \gamma_2^\mu + F_T \sigma_1^{\mu\nu} \sigma_{2\mu\nu}. \quad (6)$$

The five, complex amplitudes in Eq. (6) were obtained from the SP89 NN Wolfenstein amplitudes using Eq. (18) in Ref. 5. The form for  $F$  assumed in Eq. (6) is by no means unique. However, for the nuclei and energies being discussed here, the RIA results are very similar to the relativistic IA2 results of Ref. 6, which are based on covariant meson-exchange theory together with the use of a very general form for the NN Lorentz invariant amplitudes. The relativistic NN  $t$  matrix in the proton-nucleus center-of-momentum system with Breit frame kinematics was then obtained from Eq. (20) in Ref. 5 and used to generate the proton-nucleus optical potential.

For spin-zero targets the nuclear part of the resulting first-order RIA optical potential has the form

$$U_{\text{RIA}}^{(1)} = U_S(q) + U_V(q)\gamma^0 - 2i\alpha \cdot \mathbf{U}_T(q), \quad (7)$$

with  $\gamma^0$  the usual timelike component of the four-component Dirac  $\gamma$  matrix,  $\alpha$  the usual Dirac vector matrix,

$$U_{j=S,V}(q) = \sum_{i=p,n} t_{pi}^j(q) \bar{p}_i^j(q) \quad (8)$$

and

$$\mathbf{U}_T(q) = -i \sum_{i=p,n} t_{pi}^T(q) \nabla_q \tilde{\rho}_i^T(q). \quad (9)$$

In Eqs. (8) and (9),  $t_{pi}^j(q)$  is the relativistic NN  $t$  matrix while  $\tilde{\rho}_i^j(q)$  are momentum-space Fourier transforms of the scalar, vector and tensor (SVT) nuclear matter densities.<sup>5</sup> The vector densities  $\rho_{i=p,n}^V(r)$  were identical to those used in the NR calculations, while the scalar densities were constructed according to the prescription

$$\rho_i^S(r) = \rho_i^V(r) + [\rho_i^S(r) - \rho_i^V(r)]_{\text{RMF}}, \quad (10)$$

where the relativistic mean-field (RMF) densities used as a guide in the construction of  $\rho_i^S(r)$  were those of Horowitz and Serot.<sup>28</sup> The tensor densities used in Eq. (9) were taken directly from Ref. 28.

The static proton-nucleus Coulomb potential,  $U_C$ , adds to the vector term in Eq. (7). The anomalous magnetic moment contribution was included as an additional tensor potential of the form (in coordinate space),<sup>5</sup>

$$-i \frac{\kappa_p}{2M_p} \boldsymbol{\alpha} \cdot \hat{\mathbf{r}} \frac{\partial}{\partial r} U_C(r),$$

where  $\kappa_p$  is the additional factor required to give the proton its correct magnetic moment ( $\kappa_p = 1.79$ ), and  $M_p$  is the proton mass. The main effect of the often-omitted nuclear tensor potential [Eq. (9)] on  $Q$  and  $A_y$ , for the lighter target nuclei, is to reduce the overall magnitude of the RIA predicted values slightly, generally by less than 0.03. For the medium and heavier target nuclei, the nuclear tensor potential enhances the structure in  $A_y$  and  $Q$  slightly, by making the minima slightly deeper, generally by amounts ranging from 0.03 to 0.1. Its effects for medium to heavy target nuclei are smaller than and distinctively different from those of the anomalous magnetic moment contribution, and not confined to a particular angular region. All of the resulting RIA-Dirac equation predictions of  $A_y$  and  $Q$  observables, using Eq. (7), are shown as dashed curves in the figures.

The Dirac equation was numerically integrated out to 25 fm, including up to 180 partial waves. Because the Dirac solutions are matched to Dirac Coulomb state functions, which include the point-proton portion of the EMSO effect, convergence problems were not as severe for the Dirac solutions as for the Schrödinger equation solutions. Even so, in both approaches, we are matching at a large but finite radius (20–25 fm) to asymptotic Coulomb solutions that do not include the full EMSO effect, and as a consequence there are small, unphysical oscillations in both Dirac and Schrödinger predictions for  $A_y$  and  $Q$  for  $p + {}^{40}\text{Ca}$  at 800 MeV for angles greater than 20°, for  $p + {}^{208}\text{Pb}$  at 650 MeV for angles greater than 25°, and at 800 MeV for angles greater than 17°, as seen in Fig. 3. (Similar unphysical oscillations show up in the Schrödinger and Dirac calculation results as plotted in Ref. 8.) Since the effects on  $A_y$  and  $Q$  of the electromagnetic spin-orbit term, with which we are mainly concerned in the present work, show up most dramatically at small angles (0 to 15°), we have not carried out the extensive modifications to the Schrödinger and Dirac comput-

er programs that would be necessary in order to integrate out to the ten or more times larger matching radii required to eliminate these small, back-angle oscillations.

### III. DISCUSSION OF RESULTS

Figure 1 shows the results of the NR and RIA calculations for  $p + {}^{16}\text{O}$  at 650 and 800 MeV. Here predictions of the nonrelativistic model with electromagnetic spin-orbit potential, correlations and medium corrections (solid curves in all figure), hereinafter referred to as “NR-EMSO” calculations, are quite similar to those of the RIA (dashed curves in all figures). NR calculations which do not include the EMSO potential are shown for comparison as dash-dot curves (in all figures). The effects of the EMSO potential are fairly small at both energies, except for  $Q$  at 800 MeV, near the first maximum at 12°. The description of  $A_y$  at 650 and 800 MeV is slightly better for the NR-EMSO than for the RIA while the two descriptions of the 650 MeV  $Q$  data and the forward angle 800 MeV  $Q$  data are comparable. The NR-EMSO description of the larger angle 800 MeV  $Q$  data is significantly better than that provided by the RIA; the RIA predicts a deep minimum at 22° that does not exist in the data. The 650 MeV data are from Ref. 29, the 800 MeV data from Refs. 8 and 30. The  $Q$  data shown for 650 MeV have been reconstructed from the data for related parameter  $\beta$  shown in Ref. 29, using the corresponding  $A_y$  data, with error in  $Q$  taken as proportional to the quoted error in  $\beta$ .

Figure 2 shows the results for  $p + {}^{40}\text{Ca}$ , also at 650 and 800 MeV. In the vicinity of the first sharp structure in  $A_y$  (around 8° at 650 MeV, 7.5° at 800 MeV), the EMSO potential is indispensable in providing a realistic description. Indeed, the NR-EMSO and RIA results are quite similar at all angles, particularly at 650 MeV. The predictions of both models provide an overall, quantitative representation of the  $A_y$  data, when the electromagnetic spin-orbit term is included. For the  $Q$  data, the NR-EMSO and RIA predictions are also quite similar, with the RIA being somewhat larger at all angles and in very slightly better agreement with the data forward of 15°. Without the EMSO term at 800 MeV, the NR calculations are seen to be unable to provide enough structure in  $Q$ , at the first maximum at about 7.5°, to come anywhere near the experimental data. Overall, the quality of the fit to the data is virtually the same for both NR-EMSO and RIA models, and good overall. The data for 650 MeV are from Ref. 29, while those for 800 MeV are from Refs. 8 and 31.

Finally, in Fig. 3, the results for  $p + {}^{208}\text{Pb}$  at 650 and 800 MeV are shown. The RIA provides a better description of  $A_y$  at 650 MeV, with the NR-EMSO prediction having a bit too much structure, whereas the NR-EMSO provides a better description of the 800 MeV  $A_y$  data, the RIA prediction not having enough structure. The NR predictions omitting the EMSO potential are very poor for both energies. The structure predicted for  $A_y$  is not only washed out, but out of phase with the data, for angles less than 15°. It is not surprising that the largest effects of the EMSO term are seen for the target nucleus

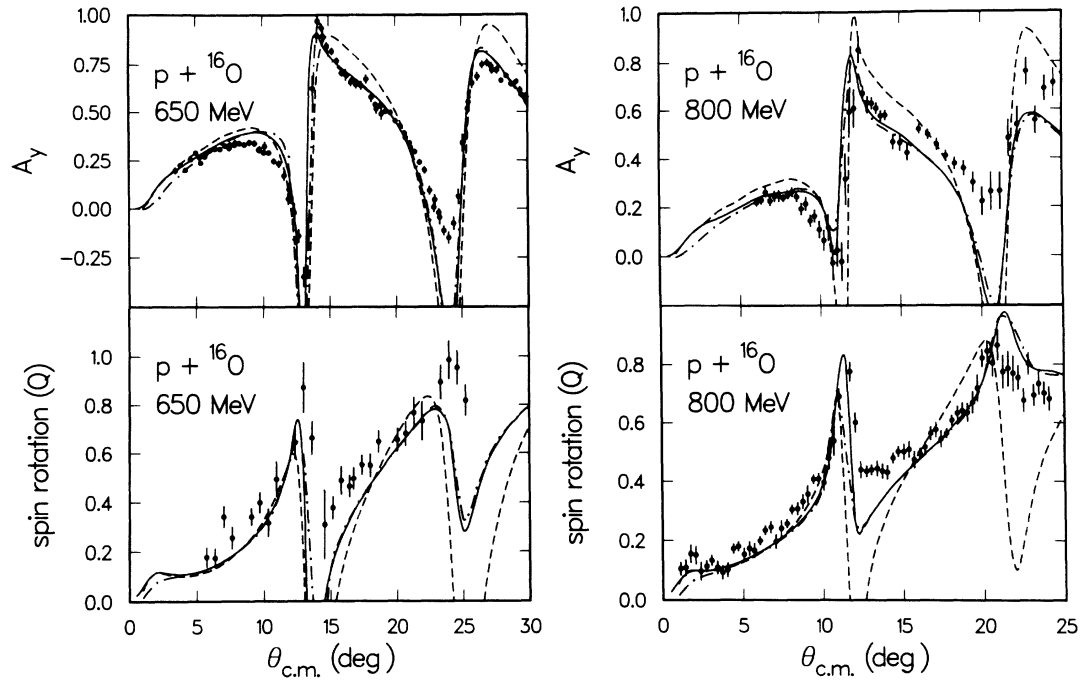


FIG. 1. Analyzing power,  $A_y$ , and spin rotation,  $Q$ , for proton elastic scattering from  $^{16}\text{O}$  at 650 and 800 MeV. The 650 MeV data are from Ref. 29, the 800 MeV data from Refs. 8 and 30. The solid curves are the nonrelativistic (NR) predictions, including electromagnetic spin-orbit (EMSO) potential, medium modifications, and correlations. The dashed curves are the Dirac (RIA) predictions. The dot-dashed curves are NR predictions without the EMSO potential, but including correlations and medium modifications.

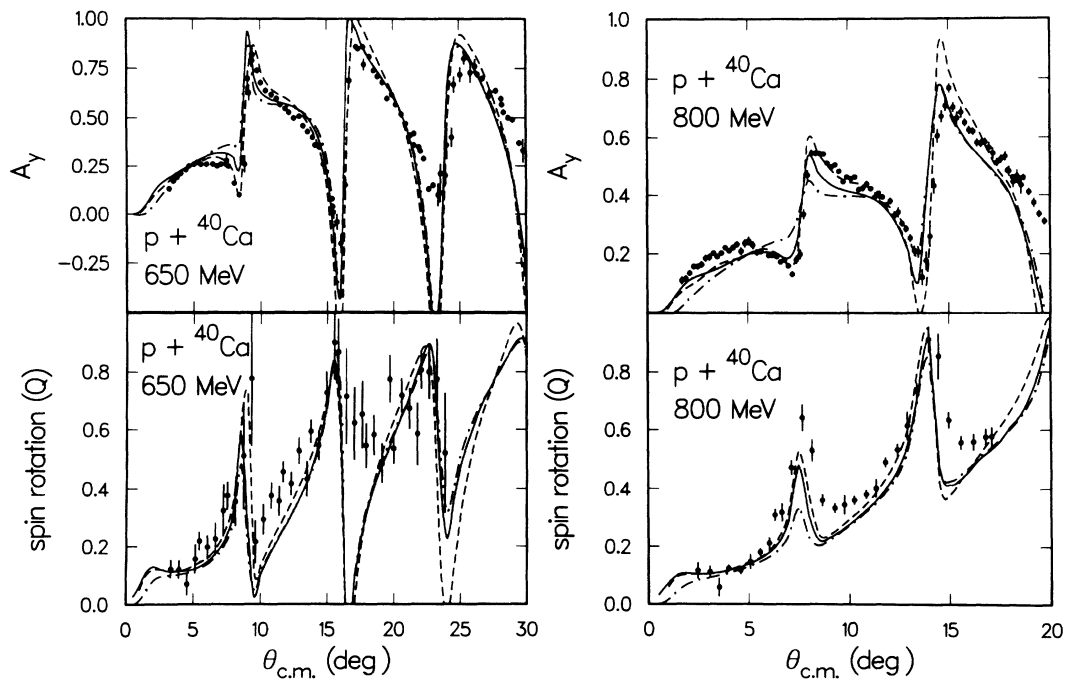


FIG. 2. Analyzing power,  $A_y$ , and spin rotation,  $Q$ , for proton elastic scattering from  $^{40}\text{Ca}$  at 650 and 800 MeV. The 650 MeV data are from Ref. 29, the 800 MeV data from Refs. 8 and 31. (See the text for explanation of how  $Q$  data at 650 MeV were generated.) The meaning of the curves is the same as in Fig. 1.

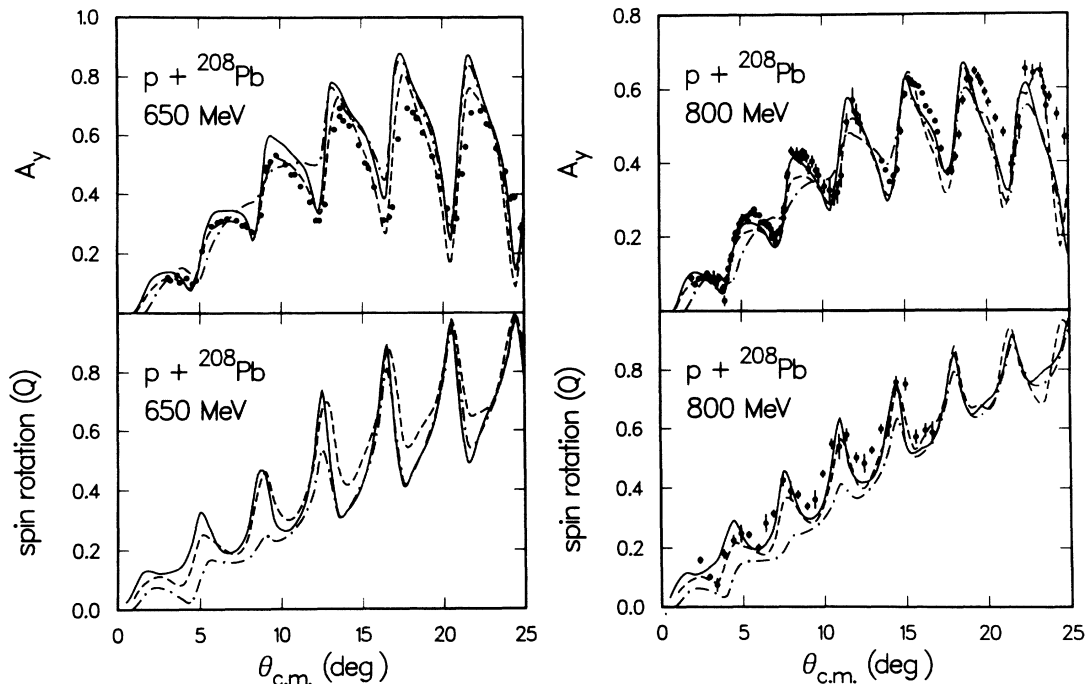


FIG. 3. Analyzing power,  $A_y$ , and spin rotation,  $Q$ , for proton elastic scattering from  $^{208}\text{Pb}$  at 650 and 800 MeV. The 650 MeV data are from Ref. 32, the 800 MeV data from Refs. 8 and 11. The meaning of the curves is the same as in Figs. 1 and 2.

with the largest charge.

The RIA predictions for  $Q$  have less structure at forward angles, compared to the NR-EMSO predictions, at both energies. The 800 MeV  $Q$  data do not provide a fine enough mesh for critical comparisons, but seem to be fit slightly better by the NR-EMSO. However, both models provide good descriptions of the available data. The NR predictions omitting the EMSO term show almost no structure for angles less than  $15^\circ$ , at either energy, and bear little resemblance to the data. The experimental data for 650 MeV are from Ref. 32, while those for 800 MeV are from Refs. 8 and 11.

Our results lead to the following general observations concerning description of  $A_y$  and  $Q$ . (1) Both the RIA and the NR-EMSO models provide very similar and equally good overall predictions for the 650 and 800 MeV data. (2) For  $^{208}\text{Pb}$ , the EMSO potential accounts almost totally for the very drastic improvement in the first-order NR-EMSO predictions at forward angles. (3) For  $^{40}\text{Ca}$ , the EMSO potential accounts for roughly half of the improvement seen, with the remainder due to inclusion of medium effects and correlations.<sup>10</sup> (4) For  $^{16}\text{O}$ , much of the improvement over lowest-order NR-EMSO calculations for  $A_y$  is due to correlations<sup>8,21</sup> and medium effects,<sup>10</sup> whereas for  $Q$ , especially at 800 MeV, the EMSO potential still plays a significant role in providing agreement with the data at the first peak at  $12^\circ$ . (5) The 800 MeV  $A_y$  and  $Q$  RIA predictions display an erroneous mass dependence, such that the curves for  $^{16}\text{O}$  have *too much* structure, those for  $^{40}\text{Ca}$  agree well with the data, while the  $A_y$  prediction (at least) for  $^{208}\text{Pb}$  has *too little* structure. (6) The NR-EMSO predictions do *not* display such

erroneous trends.

The quality of the predictions as compared to data, and the improvements obtained when various effects are included, of course depend upon the theoretical model being used, and on the approximations adopted in the calculations. However, it is important to realize that the EMSO effect, being electromagnetic in origin, is not subject to the much stronger model dependence familiar in descriptions of the strong nucleon-nucleus interaction. Note that, for instance, while correlations and medium modifications<sup>6,7,10,21,22</sup> have very different effects in the RIA and NR-EMSO, the effects of the EMSO potential are very similar in both approaches. (A good display of the effects of the EMSO potential in the RIA is found in Figs. 6 and 8 of Ref. 8, where results of calculations with a point-proton magnetic moment are compared to those with the full, anomalous magnetic moment.) In terms of the NR-EMSO model used here, we therefore see no reason why inclusion of further corrections (e.g., off-shell and full-folding effects<sup>27</sup>) should qualitatively affect our conclusions concerning the importance of the EMSO contribution. Likewise, for the RIA model, correlations, medium corrections and off-shell effects<sup>6,7,22</sup> are unlikely to affect our conclusions, or those of Ref. 8, qualitatively.

The differential cross-section predictions (not shown) are negligibly affected by the EMSO potential and medium corrections. The 800 MeV SP89 NN amplitudes predict slightly smaller magnitudes for the differential cross sections compared to results using the older SP82 solution, shown in Refs. 8 and 10. The RIA and NR-EMSO predictions at 800 MeV are therefore essentially the same as shown in Fig. 3 of Ref. 8, except for a slight reduction

in overall magnitude. The NR-EMSO differential cross-section predictions for 650 MeV are very nearly the same as shown in Ref. 10. The corresponding RIA predictions are also very similar, except that the diffractive minima for  $^{16}\text{O}$  and  $^{208}\text{Pb}$  are less deep, resulting in somewhat improved descriptions of the available data.

In general, the differential cross-section predictions of both models are fairly satisfactory, but the diffractive oscillations are shifted very slightly to smaller angles relative to the data. This indicates that the overall radial extent of the imaginary, spin-independent optical potential is a bit too large (by about 0.1–0.2 fm) in both models. This mysterious problem is discussed further in Refs. 5 and 10.

At 800 MeV the RIA differential cross-section predictions display an unrealistic mass dependence, so that the predictions for  $^{208}\text{Pb}$  are in good agreement with data, but for  $^{16}\text{O}$  become too small in overall magnitude, with minima which are much too deep. It is interesting that a similar, though much less severe, trend is seen in the NR-EMSO predictions. This unrealistic dependence of the relativistic results on target mass is not observed at 650 MeV.

The effects of the EMSO potential are, in general, less important at lower energies and for lighter nuclei. However, including this potential in NR calculations at 500 MeV, for instance those in Ref. 10 which already include medium corrections and correlations, would provide further improvement in the description of data. The NR differential cross-section and  $A_y$  predictions would, however, remain inferior to those made by the RIA. The NR density-dependent predictions for the spin rotation observables at 500 MeV are comparable to those of the RIA for  $^{16}\text{O}$ , and  $^{40}\text{Ca}$ , but remain inferior for  $^{208}\text{Pb}$ . An EMSO contribution would be expected to improve the NR spin rotation prediction for 500 MeV  $p + ^{208}\text{Pb}$ . We feel that further studies of the NR model predictions at 500 MeV would need to include the EMSO potential, along with such off-shell and full-folding effects as discussed in Refs. 24–27, which are currently believed to be significant at this and lower energies.

#### IV. CONCLUDING SUMMARY

In this work we pointed out that a part of the success of the RIA-Dirac equation model in describing proton-

nucleus elastic-scattering data at 650 and 800 MeV, for medium to heavy nuclei, is due to the automatic inclusion of electromagnetic effects involving a portion of the projectile proton's magnetic moment. We went on to show that, for the models under consideration, generally equivalent and fairly good descriptions of the 650 and 800 MeV  $A_y$  and  $Q$  data can be obtained from both the relativistic Dirac equation approach and the nonrelativistic Schrödinger equation approach, provided the EMSO potential associated with the full proton magnetic moment is included in both calculations, and the NR calculation also includes correlations and nuclear medium corrections. Based on the standard set of approximations used in implementation of the NR and RIA models, we found that including the electromagnetic coupling associated with the full projectile proton magnetic moment resulted in generally improved descriptions of the spin observable data. Most of the improvement in the lowest-order NRIA predictions at forward angles for  $^{40}\text{Ca}$  and  $^{208}\text{Pb}$  is due to the EMSO correction, although it is less important for  $^{16}\text{O}$ . Furthermore, the unrealistic mass dependence in the 800 MeV RIA spin observable predictions (seen primarily in  $A_y$ ) is not observed in the NR-EMSO calculations. Finally, the problem of explaining the angular positions of the diffractive minima in the differential cross sections persists. While the successes of both the RIA and NR-EMSO models, of course, depend on the standard approximations made in carrying out the calculations, we do not expect qualitative changes in the conclusions drawn here, concerning the importance of an *electromagnetic* spin-orbit potential, as our description of *nuclear* processes becomes more sophisticated. It is hoped that this work will help to motivate such further improvements in both the nonrelativistic and relativistic scattering models.

#### ACKNOWLEDGMENTS

This research was supported in part by the U.S. Department of Energy. The research of one of us (W.R.C.) was supported by a Faculty Research Assignment from the University Research Institute of The University of Texas at Austin.

\*BITNET addresses of the authors: COKER@UTAPHY, RAY@UTAPHY.

<sup>1</sup>A. K. Kerman, H. McManus, and R. Thaler, *Ann. Phys. (N.Y.)* **8**, 551 (1959).

<sup>2</sup>K. M. Watson, *Phys. Rev.* **89**, 575 (1953).

<sup>3</sup>J. A. McNeil, L. Ray, and S. J. Wallace, *Phys. Rev. C* **27**, 2123 (1983).

<sup>4</sup>J. Shepard, J. A. McNeil, and S. J. Wallace, *Phys. Rev. Lett.* **50**, 1443 (1983); B. C. Clark, S. Hama, R. L. Mercer, L. Ray, and B. D. Serot, *ibid.* **50**, 1644 (1983).

<sup>5</sup>L. Ray and G. W. Hoffmann, *Phys. Rev. C* **31**, 538 (1985).

<sup>6</sup>N. Ottenstein, S. J. Wallace, and J. A. Tjon, *Phys. Rev. C* **38**, 2272 (1988); *ibid.* **38**, 2289 (1988); S. J. Wallace (private com-

munication).

<sup>7</sup>D. P. Murdock and C. J. Horowitz, *Phys. Rev. C* **35**, 1442 (1987).

<sup>8</sup>R. W. Ferguson *et al.*, *Phys. Rev. C* **33**, 239 (1986).

<sup>9</sup>H. V. von Geramb, in *The Interaction Between Medium Energy Nucleons in Nuclei (Bloomington, 1982)*, Proceedings of the Workshop on the Interactions Between Medium Energy Nucleons in Nuclei, AIP Conf. Proc. No. 97, edited by H. O. Meyer (AIP, New York, 1983), p. 44; L. Rikus, K. Nakano, and H. V. von Geramb, *Nucl. Phys.* **A414**, 413 (1984).

<sup>10</sup>L. Ray, *Phys. Rev. C* **41**, 2816 (1990).

<sup>11</sup>G. M. Hoffmann *et al.*, *Phys. Rev. C* **24**, 541 (1981).

<sup>12</sup>I. Sick and J. S. McCarthy, *Nucl. Phys.* **A150**, 631 (1970).

- <sup>13</sup>I. Sick, J. B. Bellicard, J. M. Cavedon, B. Frois, M. Huet, P. Leconte, P. X. Ho, and S. Platchkov, *Phys. Lett.* **88B**, 245 (1979).
- <sup>14</sup>B. Frois, J. B. Bellicard, J. M. Cavedon, M. Huet, P. Leconte, P. Ludeau, A. Nakada, P. Z. Hô, and I. Sick, *Phys. Rev. Lett.* **38**, 152 (1977).
- <sup>15</sup>J. Dechargè and D. Gogny, *Phys. Rev. C* **21**, 1568 (1980); J. Dechargè, M. Girod, D. Gogny, and B. Grammaticos, *Nucl. Phys.* **A358**, 203c (1981); J. Dechargè (private communication).
- <sup>16</sup>R. A. Arndt (private communication); R. A. Arndt, J. S. Hyslop III, and L. D. Roper, *Phys. Rev. C* **35**, 128 (1987).
- <sup>17</sup>L. Ray, G. W. Hoffmann, and R. M. Thaler, *Phys. Rev. C* **22**, 1454 (1980).
- <sup>18</sup>C. Lechanoine, F. Lehar, F. Perrot, and P. Winternitz, *Nuovo Cimento* **56**, 201 (1980).
- <sup>19</sup>J. D. Bjorken and S. D. Drell, *Relativistic Quantum Mechanics* (McGraw-Hill, New York, 1964), p. 61.
- <sup>20</sup>B. C. Clark, S. Hama, J. A. McNeil, R. L. Mercer, L. Ray, G. W. Hoffmann, B. D. Serot, J. R. Shepard, and S. J. Wallace, *Phys. Rev. Lett.* **51**, 1808 (1983).
- <sup>21</sup>L. Ray, *Phys. Rev. C* **19**, 1855 (1979). Since the second-order Watson optical potential is  $A/(A-1)$  times the second-order KMT potential evaluated using the Watson nucleon-nucleon  $t$  matrix, the expressions given by Ray for the second-order KMT potential are easily transcribed over to the second-order Watson potential, which we used in our present calculations.
- <sup>22</sup>J. D. Lumpe and L. Ray, *Phys. Rev. C* **35**, 1040 (1987).
- <sup>23</sup>R. J. Glauber, in *Lectures in Theoretical Physics*, edited by W. E. Brittin and L. G. Dunham (Interscience, New York, 1959), p. 315.
- <sup>24</sup>K. Nakayama and W. G. Love, *Phys. Rev. C* **38**, 51 (1988); H. F. Arellano, F. A. Brieva, and W. G. Love, *Phys. Rev. Lett.* **63**, 605 (1989).
- <sup>25</sup>H. F. Arellano, F. A. Brieva, and W. G. Love, *Phys. Rev. C* **41**, 2188 (1990).
- <sup>26</sup>Ch. Elster and P. C. Tandy, *Phys. Rev. C* **40**, 881 (1989).
- <sup>27</sup>Ch. Elster, T. Cheon, E. F. Redish, and P. C. Tandy, *Phys. Rev. C* **41**, 814 (1990).
- <sup>28</sup>C. J. Horowitz and B. D. Serot, *Nucl. Phys.* **A368**, 503 (1981).
- <sup>29</sup>E. Bleszynski *et al.*, *Phys. Rev. C* **37**, 1527 (1988); C. A. Witten, Jr. (private communication).
- <sup>30</sup>G. S. Adams *et al.*, *Phys. Rev. Lett.* **43**, 421 (1979).
- <sup>31</sup>L. Ray, G. W. Hoffmann, M. Barlett, J. McGill, J. Amann, G. Adams, G. Pauletta, M. Gazzaly, and G. S. Blanpied, *Phys. Rev. C* **23**, 828 (1981).
- <sup>32</sup>N. Hintz, J. Amann, M. Barlett, D. Cook, M. Franey, K. Jones, A. Mack, G. Pauletta, B. Andrews, D. Ciskowski, L. Ping, and M. Purcell (unpublished); N. M. Hintz, University of Minnesota Summary Progress report, 1987, p. 95; N. M. Hintz, University of Minnesota Progress Report, 1989.